

## Spin triplet superconductivity in $\text{Sr}_2\text{RuO}_4$

KAROL I. WYSOKIŃSKI<sup>1</sup>, G. LITAK<sup>2</sup>, J.F. ANNETT<sup>3</sup>, B.L. GYÖRFFY<sup>3</sup>

<sup>1</sup>*Institute of Physics, M. Curie – Skłodowska University, ul. Radziszewskiego 10, 20-031 Lublin, Poland*

<sup>2</sup>*Department of Mechanics, Technical University of Lublin, Nadbystrzycka 36, 20-618 Lublin, Poland*

<sup>3</sup>*H.H. Wills Physics Laboratory, University of Bristol, Tyndall Ave, Bristol, BS8 1TL, UK*

(Submitted May 06, 2002)

Subject classification: 74.70.Pq, 74.20.Rp, 74.25.Bt

### Abstract

$\text{Sr}_2\text{RuO}_4$  is at present the best candidate for being a superconducting analogue of the triplet superfluidity in  $^3\text{He}$ . This material is a good (albeit correlated) Fermi liquid in the normal state and an exotic superconductor below  $T_c$ . The mechanism of superconductivity and symmetry of the order parameter are the main puzzling issues of on-going research. Here we present the results of our search for a viable description of the superconducting state realised in this material. Our calculations are based on a three-dimensional effective three-band model with a realistic band structure. We have found a state with non-zero order parameter on each of the three sheets of the Fermi surface. The corresponding gap in the quasi-particle spectrum has line or point nodes on the  $\alpha$  and  $\beta$  sheets and is complex with no nodes on the  $\gamma$  sheet. This state describes remarkably well a number of existing experiments including power low temperature dependence of the specific heat, penetration depth, thermal conductivity etc. The stability of the state with respect to disorder and different interaction parameters are also analyzed briefly.

**Introduction.** The discovery of superconductivity in  $\text{Sr}_2\text{RuO}_4$  [1, 2] has generated renewed interest in this material [3]. Originally the main motivation in Ref. [1] was the close similarity of its crystal structure with that of high temperature superconducting oxide  $\text{La}_{2-x}\text{Ca}_x\text{CuO}_4$ . However, unlike cuprates, strontium ruthenate is metallic without doping and is not readily superconducting. Indeed, very pure single crystals have superconducting transition temperature  $T_c = 1.5\text{K}$ , rather low on the scale of the high  $T_c$  cuprates.

In the normal state the electrons in strontium ruthenate form a well behaved, albeit anisotropic and correlated, Fermi liquid. In particular the resistivity shows a typical quadratic dependence on temperature  $\rho_i(T) = \rho_i^0 + A_i T^2$  at low temperatures. Here  $\rho_i^0$  is the ‘residual’ resistivity measured at temperature just above  $T_c$  and  $i$  denotes the direction of the current ( $i = ab$  for in plane and  $i = c$  for c-axis resistivity). Electronic transport is very anisotropic with the ratio of  $\rho_c/\rho_{ab}$  exceeding 500. Normal state electronic specific heat shows a typical linear dependence on temperature,  $C_e = \gamma T$ , with a high value of  $\gamma = 37.5 \text{ mJ/K}^2 \text{ mol}$ . The appreciable enhancement (factor 3-5) of  $\gamma$  over the band structure calculations indicates the existence of strong carrier correlations in the system. The same conclusion can also be drawn from the enhanced value of the ratio between Pauli spin-susceptibility and  $\gamma$  (Wilson ratio) and the so called Kadowaki-Woods ratio of the coefficient  $A_{ab}$  to  $\gamma$ . These values exceeds those for non-correlated systems.

Consistent with the above picture is the fact that first-principles calculations based on the Local Density Approximation (LDA) give a good qualitative account of the electronic structure [4]. The energy spectrum around the Fermi level of strontium ruthenate is dominated by electrons occupying  $t_{2g}$  orbitals ( $d_{xz}, d_{yz}, d_{xy}$ ) of  $\text{Ru}^{4+}$ . The Fermi surface consists of three

cylindrical sheets open in the  $z$ -direction. Those called  $\alpha$  and  $\beta$  stem from hybridised  $d_{xz}$  and  $d_{yz}$  orbitals, while the  $\gamma$  sheet is mainly of  $d_{xy}$  character. The  $\alpha$  sheet is a hole Fermi surface. It is centered at the point  $X$  of the bct Brillouin zone and possesses two fold symmetry. The calculated shape of the Fermi surfaces agrees nicely with that measured *via* de Haas-van Alphen effect [5].

While the normal state, as shown above, is quite typical of a good metal, the superconducting state is very exotic. The superconducting transition temperature  $T_c$  is strongly suppressed by even small amount of impurities [6]. The NMR measured relaxation rate shows no Hebel-Slichter peak, and the  $\mu$ SR experiments indicate the appearance of spontaneous magnetic fields at  $T < T_c$ . Together with a temperature independent Knight shift, all that points towards very unconventional, presumably spin-triplet, and superconductivity with a time reversal symmetry breaking pairing state.

Because the electrons forming Cooper pairs in superconductors are fermions, the pair wave function has to be odd with respect to interchange. It consists of spin and orbital components. If the total spin of a pair is zero then such a pairing state is called spin-singlet. The corresponding spin-wave function is odd so the orbital part has to be even. In Galilean invariant systems they correspond to even values of the orbital quantum number  $l = 0, 2, \dots$  and the corresponding superconducting states are referred to as having  $s$ -,  $d$ -,  $\dots$  wave symmetry. The  $s$ -wave symmetry is realised in conventional superconductors, while  $d$ -wave is the case in high temperature superconductors. The electrons in strontium ruthenate most probably pair in relative spin triplet state. Their spin wave function is even and thus the orbital one has to be odd. Even though a crystal has only discrete rotational symmetry, the corresponding symmetries of the superconducting state are still called  $p$ -,  $f$ -,  $\dots$  wave.

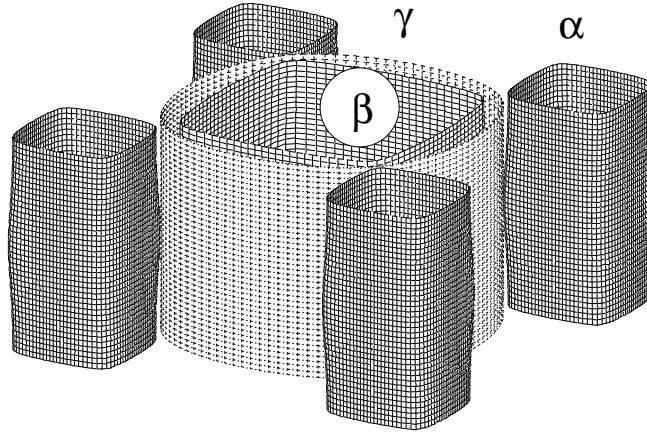


Figure 1: Calculated tight binding Fermi surface of  $\text{Sr}_2\text{RuO}_4$ .

As well known, a relatively weak dependence of  $T_c$  on the concentration of impurities and an exponential dependence of the electron specific heat on temperature point to spin singlet  $s$ -wave superconductivity. On the other hand a power law temperature dependence of specific heat is characteristic of a superconducting gap which vanishes at points or along lines on the Fermi surface, and a dramatic decrease of  $T_c$  with impurity concentration is a signal of  $l > 0$  ‘wave’ pairing.

Table 1: Irreducible representations in a tetragonal crystal. The symbols  $X, Y, Z$  represent any functions transforming as  $x, y$  and  $z$  under crystal point group operations, while  $I$  represents any function which is invariant under all point group symmetries.

irred. reps.	basis functions	time-reversal symmetry breaking	line nodes
$A_{1g}$	$I$	No	No
$A_{1u}$	$XYZ(X^2 - Y^2)$	No	Yes
$A_{2g}$	$XY(X^2 - Y^2)$	No	Yes
$A_{2u}$	$Z$	No	Yes
$B_{1g}$	$X^2 - Y^2$	No	Yes
$B_{1u}$	$XYZ$	No	Yes
$B_{2g}$	$XY$	No	Yes
$B_{2u}$	$Z(X^2 - Y^2)$	No	Yes
$E_g$	$\{XZ, YZ\}$	Yes	Yes
$E_u$	$\{X, Y\}$	Yes	No

The puzzling behaviour of  $\text{Sr}_2\text{RuO}_4$  in the superconducting state is connected with the facts that NMR,  $\mu\text{SR}$  and related experiments indicate the realisation of the  $\Delta(\vec{k}) = e_z(k_x \pm ik_y)$  state which does not vanish at the Fermi level and that the power law temperature dependence of the specific heat [7], penetration depth [8] or thermal conductivity [9] which require the gap to vanish along lines of the Fermi surface. The point is that out of all the symmetry distinct states of a bct crystal [10] none of the odd-parity states have to be time reversal symmetry breaking and also possess gap nodes at the same time (*c.f.* table I). The various states, formally fulfilling both requirements proposed in literature [11, 12] can be shown to be the sum of symmetry allowed states with distinct transition temperatures. The single superconducting transition observed in all studied samples rules out all these proposals as the single transition could only be a result of accidental degeneracy. Instead of relying on a symmetry arguments alone, we present a methodology which is based on explicit construction of an effective pairing interaction.

Below, we shall present in Sec. 2 the model and our approach. In Sec. 3 we present the results of calculations, and finally we end with our conclusions.

**The model and the approach.** Our model of superconductivity in strontium ruthenate is motivated by the experimental facts, summarised above. The electronic structure features three Fermi surfaces, and all of them are gaped to ensure the vanishing of the specific heat at  $T = 0K$ . Further, there exists a single superconducting transition and the gap has to both break the time reversal symmetry and vanish on the lines of the Fermi surface. We shall fulfill all these constraints in the context of a realistic three dimensional band structure with parameters fitted to the known details of the Fermi surface, and assumed effective attractive interactions between electrons occupying various orbitals.

We thus take the following simple multi-band attractive Hubbard Hamiltonian:

$$\begin{aligned}
\hat{H} = & \sum_{ijmm',\sigma} ((\varepsilon_m - \mu)\delta_{ij}\delta_{mm'} - t_{mm'}(ij)) \hat{c}_{im\sigma}^\dagger \hat{c}_{jm'\sigma} \\
& - \frac{1}{2} \sum_{ijmm'\sigma\sigma'} U_{mm'}^{\sigma\sigma'}(ij) \hat{n}_{im\sigma} \hat{n}_{jm'\sigma'}
\end{aligned} \tag{1}$$

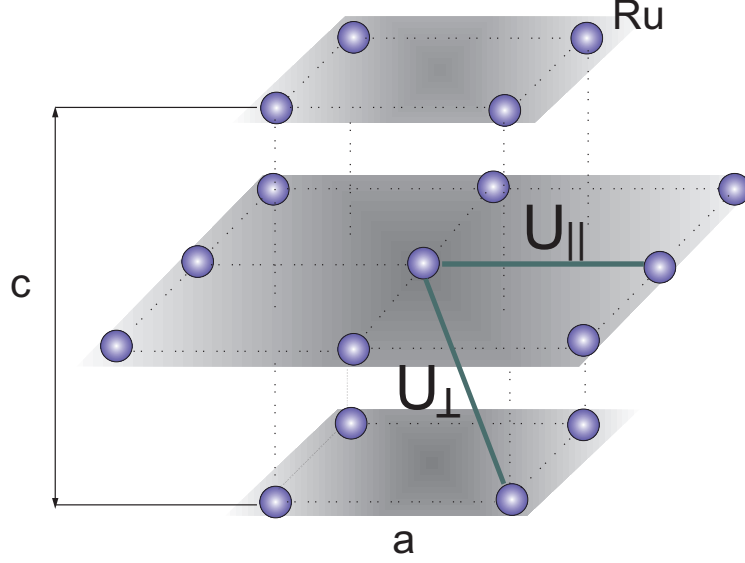


Figure 2: The relative positions of Ru ions in the tetragonal  $Sr_2RuO_4$  lattice. The heavy lines symbolise the main interactions. Interplane  $U_{\parallel}$  for the electrons occupying  $d_{xy}$  orbitals at the neighbouring in planes ions and  $U_{\perp}$  for out of plane neighbours and  $d_{xz}$  and  $d_{yz}$  orbitals.

Table 2: The values of parameters used in calculations. Here  $t, t'$  are in-plane hopping integrals between  $c$  ( $d_{xy}$ ) orbitals,  $t_{ax}, t_{bx}$  are in-plane hopping integrals between  $a$  ( $d_{xz}$ ) orbitals along  $\hat{x}$  and  $\hat{y}$  directions,  $t_{ab}$  is the in-plane hopping between  $a$  and  $b$  orbitals along  $\hat{x} + \hat{y}$ , and  $t_{hybr}$  and  $t_{\perp}$  are out of plane hopping integrals along the bct body-centre vector from  $a(b)$  to  $c$  and from  $a(b)$  to  $b(a)$ , respectively.

	$t$	$-t'$	$t_{ax}$	$t_{bx}$	$t_{ab}$	$t_{hybr}$	$-t_{\perp}$	$-\varepsilon_a$	$-\varepsilon_b$	$-\varepsilon_c$	$U_{\parallel}$	$U_{\perp}$
meV	81.6	36.7	109.4	6.6	8.8	1.1	0.3	116.2	116.2	131.8	40.3	48.2

as our model which is to describe superconductivity in  $Sr_2RuO_4$ . Here  $m$  and  $m'$  refer to the three Ruthenium  $t_{2g}$  orbitals to be denoted  $a = d_{xz}$ ,  $b = d_{yz}$  and  $c = d_{xy}$  in the following.  $i$  and  $j$  label the sites of a body centered tetragonal lattice. The hopping integrals  $t_{mm'}(ij)$  and site energies  $\varepsilon_m$  were fitted to reproduce the experimentally determined three-dimensional Fermi Surface [5, 13]. We found that the set  $t_{mm'}$  shown in Table 2 gave a good account of the data.

In choosing the interaction parameters  $U_{mm'}^{\sigma\sigma'}$  we adopted a frankly semi phenomenological approach. Namely, we eschewed any effort to derive these from an assumed physical mechanism of pairing and endeavoured to find a minimal, hopefully unique, set of parameters which describes the available data. The point of such strategy is that at the end we can claim to have identified the position and orbital dependence of the interaction and therefore provided guidance for constructing microscopic models for specific mechanisms.

In the above spirit we consider two sets of interaction constants:  $U_{mm'}^{\parallel}$  for nearest neighbours in the plane and  $U_{mm'}^{\perp}$  for nearest-neighbour Ru-atoms in the adjacent plane as indicated in Fig. 2. To limit further the parameter space we need to explore, we assume that

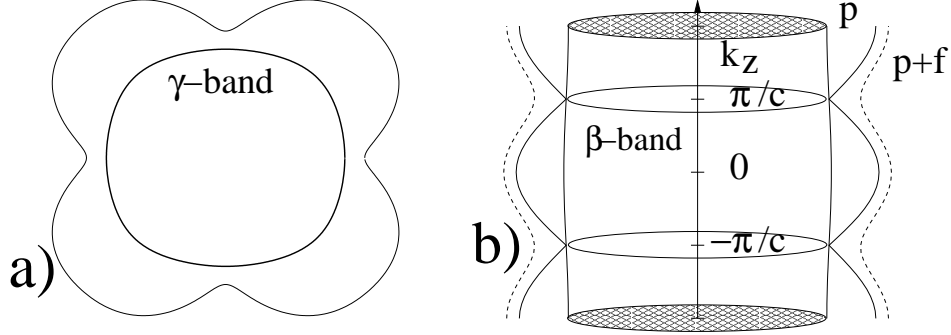


Figure 3: Lowest energy quasiparticle eigenvalues,  $E^\nu(\mathbf{k})$  on the  $\gamma$  (a) and  $\beta$  (b) Fermi surface sheets; (a) polar plot of the  $\gamma$  sheet in the plane  $k_z = 0$ ,  $E_{\gamma,max}(\mathbf{k}_F) = 0.22\text{meV}$ ,  $E_{\gamma,min}(\mathbf{k}_F) = 0.056\text{meV}$  (b) vertical cross-section of the cylindrical  $\beta$  sheet in the plane  $k_x = k_y$ ,  $E_{\beta,max}(\mathbf{k}_F) = 0.32\text{meV}$ . A non-zero  $f$ -wave order parameter (dotted line) lifts the  $p$ -wave line nodes (solid lines).

$U_{\parallel}^{cc} \equiv U_{\parallel}$ ,  $U_{\perp}^{aa} = U_{\perp}^{bb} \equiv U_{\perp}$  and contemplate only

$$U_{mm'}^{\parallel} = \begin{pmatrix} u & u & u \\ u & u & u \\ u & u & U^{\parallel} \end{pmatrix} \quad \text{and} \quad U_{mm'}^{\perp} = \begin{pmatrix} U_{\perp} & U_{\perp} & u' \\ U_{\perp} & U_{\perp} & u' \\ u' & u' & u' \end{pmatrix} \quad (2)$$

In fact, we take  $u = u' = 0$  for most of our calculations and we use only one in plane,  $U_{\parallel}$ , and one out of plane  $U_{\perp}$ , parameters to fit the experimental data on the specific heat,  $c_v(T)$ , superfluid density  $n_s(T)$  and the thermal conductivity  $\kappa_T(T)$ . The purpose of the few calculations with  $u \neq 0$ ,  $u' \neq 0$  was only to investigate the stability of the  $U_{\parallel}, U_{\perp}$  results to variations in  $U_{mm'}^{\parallel}$  and  $U_{mm'}^{\perp}$ .

Within the above model, we solved the Bogolubov-de Gennes equations:

$$\sum_{jm'\sigma'} \begin{pmatrix} E^\nu - H_{m,m'}(ij) & \Delta_{m,m'}^{\sigma\sigma'}(ij) \\ \Delta_{mm'}^{*\sigma\sigma'}(ij) & E^\nu + H_{mm'}(ij) \end{pmatrix} \begin{pmatrix} u_{jm\sigma'}^\nu \\ v_{jm'\sigma'}^\nu \end{pmatrix} = 0 \quad (3)$$

together with the self-consistency condition

$$\Delta_{mm'}^{\sigma\sigma'} = U_{mm'}^{\sigma\sigma'}(ij)\chi_{mm'}^{\sigma\sigma'}(ij); \quad \chi_{mm'}^{\sigma\sigma'}(ij) = \sum_{\nu} u_{im\sigma}^\nu v_{jm'\sigma'}^{*\nu} (1 - 2f(E^\nu)), \quad (4)$$

which follow from Eq. (1) on making the usual BCS-like mean field approximation[14]. Since  $H_{mm'}(ij)$  and  $\Delta_{m,m'}^{\sigma\sigma'}(ij)$  depend only on the difference  $\vec{R}_i - \vec{R}_j$  the solution of Eq. (3) is rendered tractable by taking its lattice Fourier transforms and, thus transforming the problem into that of a  $12 \times 12$  matrix, eigenvalue problem at each  $\mathbf{k}$  in the appropriate Brillouin Zone.

For  $u = u' = 0$  the general structure of  $\Delta_{mm'}^{\uparrow\downarrow}(\vec{k})$  turns out to be of the form

$$\begin{aligned} \Delta_{cc}(\vec{k}) &= \Delta_{cc}^x \sin k_x + \Delta_{cc}^y \sin k_y \\ \Delta_{mm'}(\vec{k}) &= \Delta_{mm'}^z \sin \frac{k_z c}{2} \cos \frac{k_x}{2} \cos \frac{k_y}{2} + \Delta_{mm'}^f \sin \frac{k_x}{2} \sin \frac{k_y}{2} \sin \frac{k_z c}{2} \\ &+ \left( \Delta_{mm'}^x \sin \frac{k_x}{2} \cos \frac{k_y}{2} + \Delta_{mm'}^y \cos \frac{k_x}{2} \sin \frac{k_y}{2} \right) \cos \frac{k_z c}{2} \end{aligned} \quad (5)$$

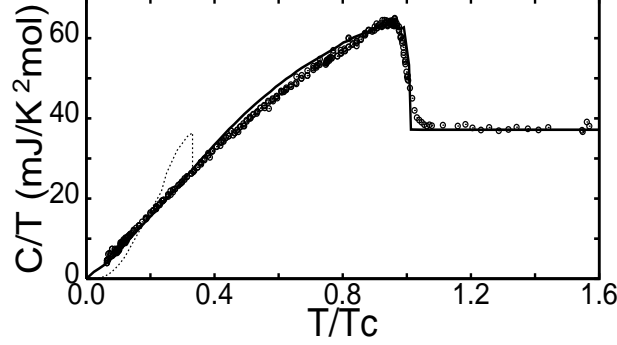


Figure 4: Calculated specific heat,  $C$ , as a function of temperature,  $T$ , compared to the experimental data of NishiZaki *et al.*[7]. The dotted-line includes the  $f$ -wave order parameter, the solid line is without  $f$ -wave.

for  $m, m' = a$  or  $b$ .

Our self-consistency procedure always converged on the amplitudes  $\Delta_{cc}^x, \Delta_{cc}^y, \Delta_{m,m'}^z(T)$ ,  $\Delta_{m,m'}^f(T)$ ,  $\Delta_{m,m'}^x(T)$  and  $\Delta_{m,m'}^y(T)$  to an accuracy higher than  $10^{-4}\%$ . The principle results of such calculations are these amplitudes and the corresponding quasiparticle energy eigenvalues  $E_\nu(\vec{k})$ . These eigenvalues are shown in Fig. 3, for the interaction values  $U_\parallel, U_\perp$  given in Table 2, and with the constraint that  $\Delta_{m,n}^f(T) = 0$ . Evidently from the figure, on the  $\gamma$  sheet there is an absolute gap below  $E_{\gamma,min}(\vec{k}_F)$ , in the quasi-particle spectrum, while the  $\beta$  sheet is gapless with a line of nodes in the gap functions at  $k_z = \pm \frac{\pi}{c}$ . This dramatically different gap structure and symmetry on different sheets of the Fermi Surface is the striking new results of an interaction matrix  $U_{mn}^{\sigma\sigma'}(ij)$  which couples electrons in different Ru-planes.

From the results in Fig. 3, one is encouraged to investigate this form of interaction further because, on the one hand, the line of zero gap on the  $\beta$  sheet explains the power-law behaviour of various thermodynamic quantities and, on the other, on the fully gapped  $\gamma$  sheet  $\Delta_{\gamma\gamma}(k) = \Delta_{cc}(k) = \Delta_{cc}^x(\sin k_x a + i \sin k_y b)$  which implies the broken time reversal symmetry demanded by a number of other experiments. Indeed, for the above pair of interactions,  $U_\perp$  and  $U_\parallel$ , and the corresponding quasiparticle spectra we find the specific heat  $c_v(T)$  shown in Fig. 4 as a function of  $T$ . Although these parameters were chosen to fit the experimental data which is also shown, the agreement between theory and experiment is truly remarkable. The point to appreciate is that in general two different  $U_\parallel$  and  $U_\perp$  imply two separate transitions at  $T_c^\parallel$  and  $T_c^\perp$ . Thus, to agree with the experiments which features a single transition at  $T_c = 1.5$  K we had to use both degrees of freedoms. Namely, fitting  $T_c$  determined both coupling constants  $U_\perp$  and  $U_\parallel$ . Now, one might suggest that it is a short-coming of our model that we have to rely on such an accidental coincidence of  $U_\parallel$  and  $U_\perp$  to fit one number  $T_c^{\text{exp}}$ . However, in the light of the very good fit to the very non trivial experimental variation of  $c_v$  with temperature this is not a strong objection. Indeed, the fact that having fitted to  $T_c^{\text{exp}}$  only and we have reproduced the slope as  $T$  goes to zero and the size of the jump at  $T_c$  has to be regarded as a confirmation of our model.

**Concluding remarks.** Our calculations [15] of the superfluid density  $n_s(T)$  [8] and thermal conductivity  $\kappa(T)$  [9], for the same parameters as above, provide further evidence in support of our model. Note that these calculations do not involve additional adjustable parameters

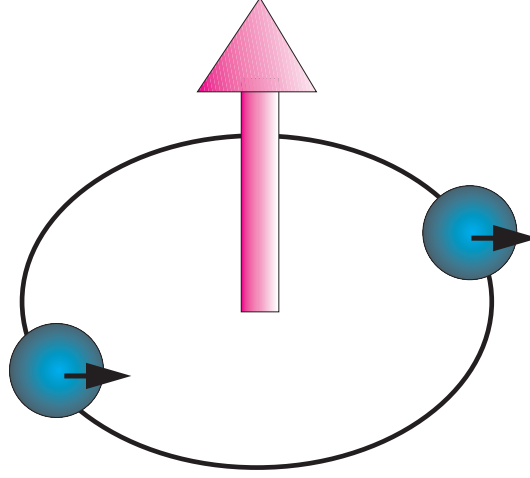


Figure 5: The structure of the order parameter. The big arrow corresponds to the orbital momentum  $l$  of the Cooper pair, while small arrows show the spins of the electrons which add to  $s = 1$ . In the frame in which  $l_z = 1$  one has  $s_z = 0$ .

and thus the results are not only qualitative consequences of nodes of the gap on the  $\alpha$  and  $\beta$  sheets of the Fermi Surface but are also quantitative predictions of the theory.

In what follows we conclude this brief survey of our very encouraging results by two further important comments. The first concerns the constraints  $\Delta_{mm'}^f(T) = 0$  imposed at each step of the selfconsistency cycle during the above calculations. Without this constraint there would be a second transition  $T_c^f < T_c$ , where  $\Delta_{m,m'}^f(T)$  becomes non zero and this would imply a peak in  $c_v(T)$  at  $T_c^f \simeq 0.2$  K, which has not been seen experimentally. Fortunately, we have been able to show by explicit quantitative calculations that a small amount of disorder will eliminate the  $\Delta_{mm'}^f$  component of the order parameters without changing the other amplitudes in Eq. (4) very much. The details of these calculations will be published elsewhere [15]. This justifies, at the present level of the mean-free path in samples on which the experiments were made, the simultaneous neglect of disorder and the  $f$ -component  $\Delta_{m,m'}^f(T)$ .

The other comment is that we have studied the stability of the above model (Eqs. 1-5, Fig. 5) to introducing further interaction constants and found it to be satisfactorily robust. In particular we have carried a number of calculations with  $u \neq 0$  and  $u' \neq 0$  and, as we shall report in a separate publication, we found [15] that the overall picture presented above remained the same. Namely, our conclusion that a model with just two interaction constants, one in plane  $U_{\parallel}$ , and one out of plane  $U_{\perp}$  (Fig. 4) roughly of the same size, around 50 meV, is capable of explaining all the available data we have analysed remained valid.

**Acknowledgments** This work has been partially supported by KBN grant No. 2P03B 106 18 and the Royal Society Joint Project.

### References

- [1] Y. Maeno, H. Hashimoto, K. Yoshida, S. NishiZaki, T. Fujuta, J.G. Bednorz and F. Lichtenberg, Nature **372**, 532 (1994).
- [2] Y. Maeno, T.M. Rice and M. Sigrist, Physics Today **54**, 42 (2001).
- [3] R.J. Cava, B. Batlogg, K. Kiyono, H. Takagi, J.J. Krajewski, W.F. Peck, Jr., L. W. Rupp, Jr., and C. H. Chen, Phys. Rev. B **49** 11890 (1994).

- [4] I.I. Mazin and D.J. Singh, Phys. Rev. Lett. **79**, 733 (1997).
- [5] A. Mackenzie and Y. Maeno, Physica **B 280**, 148 (2000).
- [6] K. Miyake and D. Narikiyo, Phys. Rev. Lett. **83**, 1423 (1999).
- [7] S. NishiZaki, Y. Maeno and Z. Mao, J. Phys. Japan **69**, 336 (2000).
- [8] I. Bonalde, B.D. Yanoff, M.B. Salamon, D.J. Van Harlingen M.E. Chia, Z.Q. Chia, and Y. Maeno, Phys. Rev. Lett. **85**, 4775 (2000).
- [9] M. A. Tanatar, M. Suzuki, S. Nagai, Z. Q. Mao, Y. Maeno, and T. Ishiguro, Phys. Rev. Lett. **86** 2649 (2001).
- [10] J.F. Annett, Adv. Phys. **39**, 83 (1990).
- [11] M.J. Graf and A.V. Balatsky, Phys. Rev. **B 62**, 9697 (2000).
- [12] T. Dahm, H. Won, and K. Maki, cond-mat/0006301.
- [13] C. Bergemann, S.R. Julian, A. P. Mackenzie, S. NishiZaki and Y. Maeno, Phys. Rev. Lett. **84**, 2662 (2000).
- [14] J.B. Ketterson and S.N. Song, *Superconductivity*, (Cambridge University Press, 1999).
- [15] J.F. Annett, B.L. Gyorffy, G. Litak, and K.I. Wysokiński, unpublished.